ISSN 0021-3640, JETP Letters, 2013, Vol. 97, No. 11, pp. 634–638. © Pleiades Publishing, Inc., 2013.
Original Russian Text © A.A. Kuzubov, N.S. Eliseeva, Z.I. Popov, A.S. Fedorov, M.V. Serzhantova, V.M. Denisov, F.N. Tomilin, 2013, published in Pis'ma v Zhurnal Eksperimental'noi i Teoreticheskoi Fiziki, 2013, Vol. 97, No. 11, pp. 732–736.

Theoretical Study of Sorption and Diffusion of Lithium Atoms on the Surface of Crystalline Silicon and inside It

A. A. Kuzubov[a, b, *], N. S. Eliseeva[a, c], Z. I. Popov[a–c], A. S. Fedorov[b, c], M. V. Serzhantova[c], V. M. Denisov[a], and F. N. Tomilin[b]

[a] *Siberian Federal University, Krasnoyarsk, 660028 Russia*

* *e-mail: alex_xx@rambler.ru*

[b] *Kirensky Institute of Physics, Siberian Branch, Russian Academy of Sciences, Akademgorodok, Krasnoyarsk, 660036 Russia*

[c] *Siberian State Aerospace University, Krasnoyarsk, 660014 Russia*

Received April 23, 2013

The energy of the sorption and diffusion of lithium atoms on the reconstructed (4 × 2) (100) silicon surface in the process of their transport into near-surface layers, as well as inside crystalline silicon, at various lithium concentrations have been investigated within the density functional theory. It has been shown that single lithium atoms easily migrate on the (100) surface and gradually fill the surface states (T3 and L) located in channels between silicon dimers. The diffusion of lithium into near-surface silicon layers is hampered because of high potential barriers of the transition (1.22 eV). The dependences of the binding energy, potential barriers, and diffusion coefficient inside silicon on distances to the nearest lithium atoms have also been examined. It has been shown that an increase in the concentration of lithium to the $Li_{0.5}Si$ composition significantly reduces the transition energy (from 0.90 to 0.36 eV) and strongly increases (by one to three orders of magnitude) the lithium diffusion rate.

DOI: 10.1134/S0021364013110088

1. INTRODUCTION

The use of silicon-based anode materials for lithium ion accumulators seems much more promising as compared to graphite-based materials standardly used in such batteries [1, 2]. The maximum concentration of sorbed lithium in silicon is reached in the $Li_{22}Si_5$ alloy, which has the highest theoretical specific capacity (4200 mA h/g) among all known anode materials [3]. At the same time, the theoretical capacity of graphite intercalated with lithium between graphite layers is only 370 mA h/g. Unfortunately, the process of the introduction of lithium atoms into silicon is accompanied by a change in the specific volume of up to 300%, as well as by phase transitions with the formation of intermediate Li_xSi_y phases. A large change in the specific volume leads to mechanical stresses and, as a result, to the total destruction of the material [4]. The solution to this problem can be the use of silicon nanostructures (nanoparticles, nanotubes, and nanowhiskers), which have a large specific surface and small volume insufficient for the destruction of a nanoparticle in the process of its recycling at sorption/desorption of lithium. The authors of [1] considered various types of silicon films and nanoparticles as candidates for an anode material. It was shown that these materials have a limited capacity and capability of keeping capacity characteristics after several charging–discharging cycles. These properties can be due to processes on the silicon surface. This is important when passing from the study of the properties of a bulk crystal to the study of the properties of thin films [5, 6].

To describe the introduction of lithium into such nanosystems whose production and measurement are very difficult, it is very important to analyze the main stages of the introduction of lithium (adsorption of lithium atoms on the surface, their penetration into near-surface layers, and their diffusion inside a crystal lattice at various concentrations of lithium) [1].

It is noteworthy that the diffusion of lithium in the bulk of silicon at its low concentrations is quite well studied in contrast to diffusion on the surface [7]. However, in contrast to bulk silicon crystals, diffusion of lithium atoms on the surface, as well as their penetration into the near-surface layers, is of particular importance.

The comparison of the average time of residence of adsorbed lithium on the (100) and (111) surfaces in [8] indicates that the diffusion of lithium into the bulk of silicon occurs primarily through the (100) surface rather than through the (111) surface. The possible reason is that the (111) surface has a closer packing than the (100) surface. For this reason, we consider plates with the (100) surface in this work. It is known that the reconstruction of the surface can strongly affect the sorption and diffusion of lithium on the silicon surface. Dimers inducing the (2 × 1) reconstruction are formed on the Si(100) surface at room temperature. The model of antisymmetric dimers that are

energetically more favorable than symmetric dimers is commonly accepted. This fact was confirmed theoretically [10] and experimentally [11]. It is worth noting that, according the calculations for the predicted antisymmetric model of dimers, the (2 × 1) Si(100) reconstruction cannot be the ground state at room temperature. The (2 × 2) or (4 × 2) surface phase can be the ground state. The transition of the (2 × 1) reconstruction to the (4 × 2) reconstruction was detected experimentally when the temperature was reduced to 200 K [11, 12]. It is noteworthy that the diffusion of lithium in silicon at finite concentrations of lithium is almost unstudied. The diffusion coefficient of lithium in silicon was obtained in [13], but the effective concentration corresponding to the measured diffusion coefficient was not determined. This can be explained by the difficulty of the measurement of the nonstationary diffusion process at a constant concentration of lithium, as well as by the rich phase diagram of Li_xSi, which can induce the rearrangement of the crystal structure even under the conditions of the electrochemical saturation of silicon with lithium [14].

The aim of this work is to study mechanisms of the sorption and diffusion of lithium atoms on the (100) silicon surface with the (4 × 2) reconstruction and the transition of lithium atoms to near-surface layers of silicon, as well as to determine the dependence of the diffusion rate of lithium inside the silicon bulk on the lithium concentration.

2. OBJECTS OF THE STUDY AND THE METHOD OF CALCULATIONS

The quantum-chemical simulation in this work was performed in the VASP 5.3 package [15–17] within the density functional theory using the plane wave basis and PAW formalism [18]. The cutoff energy of plane waves E_{cutoff} in the calculations was 245.3 eV. The calculations were performed in the generalized gradient approximation (GGA) of the Perdew–Burke–Ernzerhof exchange correlation functional [19] with the Grimme correction taking into account van der Waals interaction [20]. To determine the transient state and potential barriers for the diffusion of a lithium atom on the surface and in the Si(100) near-surface layers, we used the nudged elastic band (NEB) method [21]. When simulating all structures under study, the geometry was optimized to the maximum forces acting on atoms (0.01 eV/Å).

To study the sorption and diffusion of a lithium atom on the surface and in near-surface silicon layers, we simulated a slab with the (100) surface. The slab was a 4 × 4 × 3 supercell with the sizes $a = 15.372$ Å and $b = c = 21.543$ Å with the possibility of the (4 × 2) reconstruction of both surfaces. To exclude the effect of atoms of neighboring slabs on these surfaces, a vacuum gap of 27 Å was specified along the normal to the surface of the slab. Since the supercell is rather large, for the integration over the first Brillouin zone, the supercell was automatically divided into the uniform 2 × 2 × 1 grid chosen by the Monkhorst–Pack scheme [22]. The minimum thickness of the slab was chosen in terms of the calculated surface energy. For the silicon slab that had a thickness of 15.372 Å and consisted of three cubic unit cells, the surface energy was 151.6 meV/Å^2 in good agreement with the values of 155.9 and 149.2 meV/Å^2 obtained in [23] and [24], respectively.

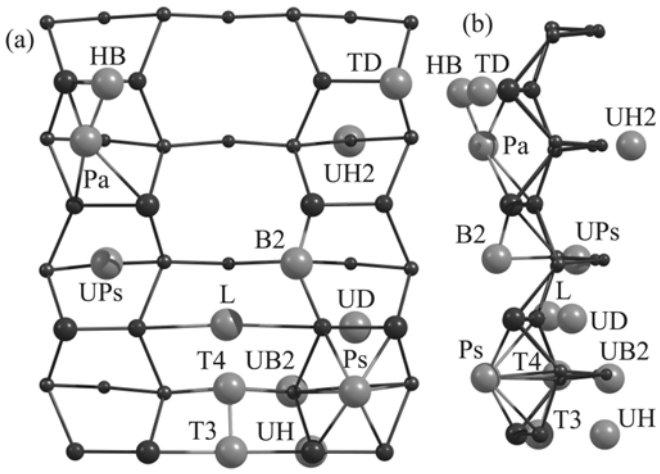

Fig. 1. (a) Plan and (b) side views of various positions of a lithium atom on the surface and in Si(100) near-surface layers (silicon and lithium atoms are given in dark and light colors, respectively).

3. STUDY OF THE ENERGY OF ADSORPTION AND DIFFUSION OF SURFACE LITHIUM ATOMS

To determine the most favorable positions of a single lithium atom on the surface and in the near-surface Si(100) layers, we calculated the structures with different positions of this atom (Fig. 1). The notation of all such positions was given in [25, 26].

The binding energy of the lithium atom with the Si(100) surface (Table 1) was calculated by the formula $E = E_{SiLi} - E_{Si} - E_{Li}$, where E_{SiLi} is the total energy of the Si(100) system with the adsorbed lithium atom, E_{Si} is the total energy of the silicon supercell with the reconstructed (100) surfaces, and E_{Li} is the energy of one lithium atom in its crystal lattice.

According to Table 1, the most energetically favorable positions of the single lithium atom are T3 and L, where this atom is in the channel between silicon dimers (Fig. 1). The Ps and B2 surface states are slightly less stable (the energy difference between them and the positions in the channel is about 0.1 eV).

It is noteworthy that the binding energy of the lithium atom with silicon decreases at the penetration of the lithium atom into the bulk (positions UD, UH,

Table 1. Binding energies of a lithium atom with the (100) Si surface for its various surface or near-surface positions

Surface	E_{bind}, eV	Near-surface	E_{bind}, eV
T3	−1.240	UPs**	−1.037
L	−1.177	UH	−0.810
T4*	−1.160	UB2	−0.809
Ps	−1.045	UH2	−0.761
B2**	−1.045	UD	−0.110
Pa**	−1.045		
HB	−0.518		
TD	−0.517		

Notes: * Lithium atom after optimization passes to the T3 position.
** Lithium atom passes to the Ps position.

Table 2. Height of the potential barrier for the direct (U_{dir}) and inverse (U_{inv}) transitions on the surface and in Si(100) near-surface layers

Migration type	Direction	U_{dir}, eV	U_{inv}, eV
On the surface	T3–L	0.43	0.37
	L–Ps	0.44	0.31
From the surface to near-surface layers	T3–UH	1.22	0.79
	Ps–UH	2.46	2.23
In near-surface layers	UH–UB2	0.78	0.85
	UH–UD	0.84	0.13

UH2, and UB2) or at its emergence from the channel on the surface (positions HB and TD). Thus, the initial location of lithium atoms in the channel between silicon dimers is preferable.

To confirm this conclusion, we simulated the motion of the lithium atom on the surface and in the near-surface Si(100) layers. The heights of the potential barriers for different migration paths of the single lithium atom are summarized in Table 2.

According to Table 2, the migration of lithium on the surface is quite easy (T3–L or L–Ps transition). However, the penetration of the lithium atom from the surface into the near-surface layers is hindered (T3–UH and Ps–UH transitions) because of high potential barriers of the transition. Therefore, it is favorable for the lithium atom to stay in the initial surface sorption state; moreover, the migration of the lithium atom into the bulk is additionally slowed owing to the high hopping barrier.

It is worth noting that the potential barriers to migration for the single lithium atom decrease in the deeper near-surface layers (UH–UB2 and UH–UD transitions). In these layers, the barrier height is comparable with the calculated (0.85 eV for the cubic cell of silicon consisting of 64 atoms) and experimental (0.8 eV) [27] values of the barrier to the migration of lithium in the silicon bulk.

4. STUDY OF THE DEPENDENCE OF THE DIFFUSION RATE OF LITHIUM INSIDE SILICON ON THE LITHIUM CONCENTRATION

At this stage, we simulated the silicon supercell consisting of 216 atoms in the form of a cube consisting of $3 \times 3 \times 3$ unit cubes. The k points for the integration over the first Brillouin zone were constructed on a $3 \times 3 \times 3$ grid. It is known [28] that lithium atoms in the crystal structure of silicon are located at the centers of tetrahedra of silicon atoms (tetrahedral pores) (T_d). The number of such pores is equal to the number of silicon atoms. To determine the potential barriers and binding energies of lithium atoms, we placed one to four lithium atoms in the supercell. Their positions were chosen so that the distance between them was minimal. Then, this initial geometry of the system was optimized. After that, one of the lithium atoms was transferred to the final position, which was the center of the neighboring tetrahedron. Then, the coordinates of the atoms were again optimized. In the case of three and four lithium atoms, the position of the lithium atom equidistant from other lithium atoms was changed. After that, the heights of the potential barrier (transient state) for the hopping of the lithium atom from the initial to final state were calculated using the nudged elastic band method and taking into account the energies E_0 of zero-point oscillations obtained by finding the phonon frequencies. These frequencies were calculated using the frozen phonon method. To calculate the force matrix, atoms were deflected from the equilibrium position by ±0.02 Å along all of the directions.

The resulting barrier heights were 0.903, 0.735, 0.477, and 0.362 eV for various numbers ($N = 1, 2, 3$) of other lithium atoms at the centers of neighboring tetrahedra. These values were used to obtain the interpolated polynomial dependence of the height of the potential barrier $V_{barrier}$ on the number P of neighboring lithium atoms: $V_{barrier} = E_{b0} - 0.07P^3 + 0.277P^2 - 0.375P$, where $E_{b0} = 0.903$ eV is the calculated $V_{barrier}$ value for the hopping of the lithium atom from a tetrahedral pore to the neighboring pore without surrounding lithium atoms.

In addition, we calculated the Li_xSi structures with x varying up to $x = 0.5$. It was found that the $Li_{0.5}Si$ system with the displacement of any lithium atom stepwise transits to a new amorphous-like state. Such a behavior is confirmed experimentally, although the concentration at which the transition to the amorphous state occurs was not determined exactly [14].

To calculate the dependence of the diffusion rate of lithium in silicon on the lithium concentration, we used an original method. It is based on the calculation

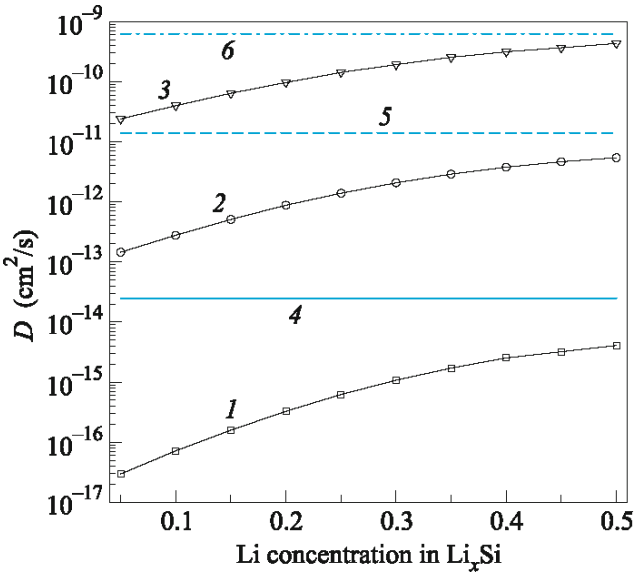

Fig. 2. Diffusion coefficient D versus the lithium concentration in Li_xSi. Lines with markers present the calculated D values at temperatures of (*1*) 300, (*2*) 400, and (*3*) 500 K. Lines without markers present the D values obtained from the experimental data reported in [13] for temperatures of (*4*) 300, (*5*) 400, and (*6*) 500 K.

of the time evolution of the distribution function of lithium atoms $P(R_i, t_n)$ defined as the probability of filling the minimum (center of the tetrahedron) with the coordinates R_i with the lithium atom at the time t_n. This evolution is described by the discrete master equation (replacing the continuous diffusion equation)

$$\frac{dP(R_i, t_n)}{dt} = \sum_{R_i} W(R_i, R_j)P(R_j, t_n)[1 - P(R_i, t_n)] - W(R_j, R_i)P(R_i, t_n)[1 - P(R_j, t_n)]. \quad (1)$$

Here, $W(R_j, R_i)$ is the frequency of hopping of an impurity atom from the minimum R_i to the minimum R_j. These quantities for the hopping of an atom through the barrier $V_{\text{barrier}}(R_i, R_j)$ at temperature T were calculated by the Arrhenius-type formula $W(R_i, R_j) = W_0\exp[-V_{\text{barrier}}(R_i, R_j)/kT]$. For the stability of the behavior of evolution $P(R_i, t_n)$, the time step τ was chosen so that its product by the maximum $W(R_i, R_j)_{\max}$ was 0.01. The pre-exponential factor (effective frequency of oscillations) W_0 was calculated by the known Vineyard formula [29]

$$W_0 = \frac{kT}{\hbar}\frac{\prod_{i=1}^{3N-3}[1 - \exp(-h\nu_i/kT)]}{\prod_{i=1}^{3N-4}[1 - \exp(-h\nu_i'/kT)]}, \quad (2)$$

where ν_i' and ν_i are the frequencies of oscillations of N atoms of the system when the transferred atom is at the saddle and minimum points, respectively. After 100 iterations of the time evolution $P(R_i, t_n)$, the diffusion coefficient D was calculated. To this end, we numerically solved the Fick equation $J = -D\partial C/\partial x$, where J is the flux, i.e., the total number of lithium atoms passing per unit time through unit area of the plane perpendicular to the axis coinciding with the direction of the gradient C of the concentration of lithium atoms in this plane. Figure 2 shows the dependences of the diffusion coefficients D on the initial concentration of lithium calculated by the described method for various temperatures. It can be seen that the diffusion coefficients calculated for various temperatures and the concentration of lithium corresponding to the $Li_{0.45}Si$ compound are in good agreement with the experimental data. Unfortunately, the effective concentrations of lithium corresponding to the measured D values cannot be determined experimentally. A strong increase (by one to three orders of magnitude) in the diffusion coefficient of lithium with an increase in its concentration to 0.45 can be explained by a sharp decrease in the potential barrier for hopping of the lithium atom to the neighboring tetrahedron in the presence of neighboring lithium atoms. This decrease can be attributed to the electrostatic repulsion of closely spaced lithium atoms, which have a partial positive charge owing to the difference between the electronegativities of lithium and silicon.

5. CONCLUSIONS

The initial stage of the adsorption of lithium atoms on the reconstructed (100) silicon surface has been studied in this work. It has been shown that lithium atoms are primarily sorbed in the surface states (T3, L) located between silicon dimers, easily migrating between them and gradually filling them. In this case, the migration of lithium atoms from the surface to the bulk of silicon is hindered because of high transition potential barriers, which decrease assumingly at a larger filling factor of the surface. The dependence of the diffusion coefficient of lithium on its concentration inside the silicon bulk has also been examined. It has been found that the heights of the potential barriers for hopping of the lithium atom with an increase in the lithium concentration decrease and, correspondingly, the diffusion coefficient increases strongly (by one to three orders of magnitude at $T \le 500$ K) with an increase in its concentration to $x = 0.5$. The experimental data according to which the further increase in the lithium concentration is accompanied by the transition of the structure to the amorphous state have been confirmed.

We are grateful to the Institute of Computational Modeling, Siberian Branch, Russian Academy of Sciences (Krasnoyarsk); the Joint Supercomputer Cen-

ter, Russian Academy of Sciences (Moscow); the Computer Center, Siberian Federal University (Krasnoyarsk); and Research Computer Center, Moscow State University, for the opportunity of using their computer clusters to perform the calculations. This work was supported by the Ministry of Education and Science of the Russian Federation (contract no. 14.V37.21.0163) and by the Russian Foundation for Basic Research (project no. 12-02-00640-a).

REFERENCES

1. U. Kasavajjula, C. Wang, and A. J. Appleby, J. Power Sources **163**, 1003 (2007).
2. G. Cohn, D. Starosvetsky, R. Hagiwara, et al., Electrochem. Commun. **11**, 1916 (2009).
3. H. Okamoto, J. Phase Equilib. **11**, 306 (1990).
4. H. Li, X. J. Huang, L. Q. Chen, et al., Solid State Ionics **135**, 181 (2000).
5. A. Magasinki, P. Dixon, B. Hertzberg, et al., Nature Mater. **9**, 353 (2010).
6. L.-F. Cui, Y. Yang, Ch.-M. Hsu, and Y. Cui, Nano Lett. **9**, 3844 (2009).
7. *Landolt-Börnstein, Semiconductors. Physics of Group IV Elements and III–V Compounds Group III* (Springer, Berlin, 1984), p. 17.
8. H. Kleine, M. Eckhardt, and D. Fick, Surf. Sci. **329**, 71 (1995).
9. M. Eckhardt, H. Kleine, and D. Fick, Surf. Sci. **319**, 219 (1994).
10. E. Kruger and J. Pollmann, Phys. Rev. B **47**, 1898 (1993).
11. L. S. O. Johansson, R. I. G. Uhrberg, E. Martensson, et al., Phys. Rev. B **42**, 1305 (1990).
12. Y. Enta, S. Suzuki, and S. Kono, Surf. Sci. **242**, 277 (1991).
13. E. M. Pell, Phys. Rev. **119**, 1222 (1960).
14. P. Limthongkul, Y. Jang, N. J. Dudney, and Y. Chiang, J. Power Sources **119–121**, 604 (2003).
15. G. Kresse and J. Hafner, Phys. Rev. B **47**, 558 (1993).
16. G. Kresse and J. Hafner, Phys. Rev. B **49**, 14251 (1994).
17. G. Kresse and J. Furthmller, Phys. Rev. B **54**, 11169 (1996).
18. P. E. Blechl, Phys. Rev. B **50**, 17953 (1994).
19. J. P. Perdew, K. Burke, and M. Ernzerhof, Phys. Rev. Lett. **77**, 3865 (1996).
20. S. Grimme, J. Comp. Chem. **27**, 1778 (2006).
21. G. Henkelman and H. Jonsson, J. Chem. Phys. **113**, 9978 (2000).
22. H. J. Monkhorst and J. D. Pack, Phys. Rev. B **13**, 5188 (1976).
23. C. Battaglia, G. Onida, K. Gaal-Nagy, et al., Phys. Rev. B **80**, 214102 (2009).
24. A. A. Stekolnikov, J. Furthmuller, and F. Bechstedt, Phys. Rev. B **65**, 115318 (2002).
25. A. Horsfield, S. Kenny, and H. Fujitani, Phys. Rev. B **64**, 245332 (2001).
26. A. A. Kuzubov, T. A. Kozhevnikova, A. S. Fedorov, et al., J. Siber. Federal Univ., Math. Phys. **3** (1), 125 (2010).
27. C. E. Allen, D. L. Beke, H. Bracht, et al., Group III: Condens. Matter **3**, 2 (1997).
28. W. Wan, Q. Zhang, Y. Cui, and E. Wang, J. Phys.: Condens. Matter **22**, 415501 (2010).
29. G. V. Vineyard, J. Phys. Chem. Solids **3**, 121 (1957).

Translated by R. Tyapaev